Laksono FX Anjar Tri (Orcid ID: 0000-0002-6061-6136)

Shoreline Change Dynamics Along the Augusta Coast, Eastern Sicily, South Italy

FX Anjar Tri Laksono

Doctoral School of Earth Sciences, Department of Geology and Meteorology, Institute of Geography and Earth Sciences, Faculty of Sciences, University of Pécs, Ifjúság u. 6, Pécs, 7624, Hungary.

Department of Geological Engineering, Faculty of Engineering, Jenderal Soedirman University, Mayjen Sungkono Rd. KM 5, Purbalingga, 53371, Indonesia

anjar93@gamma.ttk.pte.hu

Laura Borzi

Dipartimento di Scienze Biologiche, Geologiche e Ambientali, Sezione di Scienze della Terra, University of Catania, Corso Italia 57, 95129, Catania, Italy.

borzilaura@unict.it

Salvatore Distefano

Dipartimento di Scienze Biologiche, Geologiche e Ambientali, Sezione di Scienze della Terra, University of Catania, Corso Italia 57, 95129, Catania, Italy.

salvatore.distefano@unict.it

Lili Czirok

Quantectum AG, Churerstrasse 80, 8808, Pfäffikon, Switzerland

This article has been accepted for publication and undergone full peer review but has not been through the copyediting, typesetting, pagination and proofreading process which may lead to differences between this version and the Version of Record. Please cite this article as doi: 10.1002/esp.5644

Doctoral School of Roth Gyula Forestry and Wildlife Management Sciences, University of Sopron Bajcsy–Zsilinszky utca 4, 9400, Sopron, Hungary.

cziroklili@gmail.com

Ákos Halmai

Doctoral School of Earth Sciences, Department of Geology and Meteorology, Institute of Geography and Earth Sciences, Faculty of Sciences, University of Pécs, Ifjúság u. 6, Pécs, 7624, Hungary.

halmaia@gamma.ttk.pte.hu

Agata Di Stefano

Dipartimento di Scienze Biologiche, Geologiche e Ambientali, Sezione di Scienze della Terra, University of Catania, Corso Italia 57, 95129, Catania, Italy.

agata.distefano@unict.it

János Kovács

Doctoral School of Earth Sciences, Department of Geology and Meteorology, Institute of Geography and Earth Sciences, Faculty of Sciences, University of Pécs, Ifjúság u. 6, Pécs, 7624, Hungary.

jones@gamma.ttk.pte.hu

ACKNOWLEDGEMENTS

The authors would like to thank the Doctoral School of Earth Sciences, Department of Geology and Meteorology, Institute of Geography and Earth Sciences, Faculty of Sciences, University of Pecs, Hungary and Új Nemzeti Kiválóság Program (UNKP) with research grant number UNKP-22-3-1 for supporting us to conduct and publish this research.

AUTHOR CONTRIBUTIONS

FX Anjar Tri Laksono contributed in conceptualization, methodology, investigation, resources, and writing-initial draft; Laura Borzì conducted investigation, simulations using software, and writing-reviewing and editing; Salvatore Distefano contributed to the idea, interpreted the data, and wrote the manuscript; Lili Czirok performed provided resources, methodology, and writing-reviewing; Ákos Halmai provided funding acquisition, resources, and software; Agata Di Stefano provided supervision; János Kovács contributed as supervision.

DATA AVAILABILITY STATEMENT

Data sharing not applicable to this article as no datasets were generated or analysed during the current study.

CONFLICT OF INTEREST STATEMENT

The authors declare that they have no conflict of interest.

Abstract

The coastal region of Augusta, Eastern Sicily, Italy, is a densely populated zone, where human pressures profoundly shaped the coastal and land dynamics. So far, understanding the interaction between natural and human processes in modelling coastal geomorphology is still quite challenging. However, coastal and environmental monitoring poses the bases for managing coastal areas properly. Therefore, this research aim was first to understand the medium-term shoreline changes along Augusta Bay between 1972 and 2021, and then assess the main local coastal modifications determined by the increasing coastal armouring. To do so, the shorelines dataset was extracted from Landsat and Sentinel-2 satellite imageries using the NDWI and mNDWI methods and then statistical parameters were computed using Digital Shoreline Analysis System (DSAS). Results show that this coastal fringe experienced significant shoreline recession over the studied time interval. Negative shoreline shifts are higher in correspondence with torrent deltas, as a result of the increasing human and natural forces insisting on the land and coastal environments. Since 1970s, Augusta Bay registered a significant increase in artificial coastal length and a coastal armouring index of Maximal level was today reached.

Keywords: WLR, coastal armouring index, DSAS, shoreline change, Augusta

1. INTRODUCTION

Around 60% of the world's population that lives in coastal areas is vulnerable to erosional phenomena (Cai et al., 2009; Wang et al., 2021;

Zhang et al., 2021). Coastal morphology is modeled by the interaction between sediment budget and physical oceanographic conditions(Cao et al., 2020; Distefano & Gamberi, 2022; Laksono et al., 2022a; Todd et al., 2019). However, in recent times, the extensive man-made modifications of coasts and lands, i.e. ports, coastal defence structures, and human settlements, become key factors in triggering coastal dynamic changes (Chu et al., 2020; Di Stefano et al., 2013; Fletcher et al., 2012). As such, many studies on shoreline changes throughout the world have been carried out over the last few years (Bacino et al., 2020; Borzì et al., 2021; Quang et al., 2021a; Aladwani, 2022). Shoreline change analysis methods that have been applied worldwide comprise the use of video images introduced by Holman et al. (1993), Plant and Holman (1997), and Lippmann and Holman (1989), numerical modeling by applying continuity equation in LITPACK software (Rezaee et al., 2019), and computation of End Point Rate (EPR), Linear Regression Rate (LRR), and Weighted Linear Regression Rate (WLR) statistical parameters from image analysis utilizing Digital Shoreline Analysis System (DSAS) software (Johnston et al., 2023; Laksono et al., 2022b; Santos et al., 2021).

In the Mediterranean area, the long- and medium-term coastal retreat emerged to be the result of persistent sediment budget alterations, as response mainly to riverine sediment discharge decrease and longshore transport changes due to the harbours or coastal defence structures emplacement (Borzì et al., 2021). The Augusta Bay is one of the primary harbour and oil refineries areas in Italy and significantly contributes to the Italian economy (Margheriti, 2021; Selvaggi et al., 2018). Thus, this study area represents a good example of highly urbanized coastal areas to be assessed from a coastal change perspective. This research presents a novelty, an integrated approach to studying the Augusta coastal area that is based on data integration between assessments of shoreline change rates, coastal armoring, and marine climate characterization through literature reviews. Hence, this study coupled the shoreline evolution of Augusta Bay (Eastern Sicily, Italy, **Fig. 1**) within a 50-year interval (1972 – 2021) with the coastal armouring index (Aybulatov & Artyukhin, 1993) in order to detect the main coastal changes over a longer temporal period and to provide a useful tool for coastal management and shoreline prediction process.

2. Study Area: The Augusta Bay (Southern Italy)

2.1 Geological setting

The Augusta coastal area represents the northern edge of the Hyblean Plateau (Ben-Avraham & Grasso, 1991; Ben-Avraham & Ginzburg, 1990), which belongs to the submerged Pelagian Block (Burollet et al., 1978) and represents part of the emerged Africa foreland domain (Firetto et al., 2013). The Hyblean Plateau is tectonically controlled by the convergence between the African and European plates, which affected both the on- and off-shore setting of the southeastern coast of Sicily. In fact, the large-scale ongoing geological processes control the morpho-structural pattern of the

Hyblean Plateau (Maniscalco et al., 2022), and also reflect the submerged areas (Carbone et al., 1987; Distefano et al., 2018; Distefano et al., 2019a; Distefano et al., 2019b, 2021a; Distefano et al., 2021b; Firetto et al., 2013; Gamberi et al., 2019; Maniscalco et al., 2022; Pirrotta et al., 2013).

The off-shore N-S directed fault, the Malta Escarpment Fault (MEF), splits the Hyblean Plateau to the East from the Ionian Basin. Onshore strands of the MEF detected along the Ionian coast of SE Sicily give rise to incipient pull-apart grabens (Augusta and Anapo Grabens) of the Late Pliocene-Early-Pleistocene age (Carbone et al., 2011). The Augusta Basin represents a tectonic depression in the eastern part of the Hyblean Plateau and is mostly controlled by two NW–SE oriented fault lines, the NW-dipping Mt. Climiti Fault that splits the Augusta Basin from the Magnisi–St. Panagia ridge and the Mt. Tauro Fault fall within the Mt. Tauro Horst at the northern part of the basin (Bianca et al., 1999; Catalano et al., 2010). This tectonic setting is responsible for an overall regional uplift that involves the study area, with values of about 2 mm/yr in the north decreasing southward (Carbone et al., 1982; Firetto et al., 2013; Scicchitano & Monaco, 2006; Spampinato et al., 2011). Other archeological studies show minor uplift rates in the proximity of the Augusta Basin (about 0.30 mm/yr), suggesting that the area is undergoing differential displacements upon a regional, long-term uplift process (Scicchitano et al., 2008).

The Augusta Basin stratigraphy is made of a Mesozoic-Cenozoic shallow-water succession covered by a basin carbonate sedimentary succession, intercalated by volcanic rocks (Carbone et al., 2011). In detail, Lower Pleistocene calcarenites sands move upward to blue silty clays and unconformably lie on an Upper Cretaceous–Miocene succession composed of carbonates (Upper Cretaceous–Oligocene), calcarenites and rhodolites of the Mt. Climiti Fm. (Early–Middle Miocene), superimposed by the Mt. Carrubba Fm. (Late Miocene) and intercalated by coeval submarine volcanic rocks. The recent-most deposits are represented by the Upper Pleistocene sand, calcarenites, and conglomerates of the Panchina Fm. *Auct.* and by the Holocene alluvial deposits and beaches (Carbone et al., 2011) (**Fig. 2**.

2.2 Physical oceanographic conditions

The Augusta Bay is a semi-enclosed marine area where two main inlets establish connections with the open sea (Salvagio et al., 2016; Sprovieri et al., 2011), the Levantine and Scirocco inlets. The water circulation in the Levantine inlet can be mostly described by a northward tidal flowing with a mean velocity of 18 cm/s at the surface and 7 cm/s at the bottom. In the Scirocco inlet, a flowing parallel to the coast is present with a moderate velocity (8 cm/s at the surface and 4 cm/s at the bottom) at the southern part of the bay. Scarce active currents are observed in the northern part of the Augusta Bay. Even though the off-shore water circulation of the Ionian Sea is mostly NNE-directed, the nearshore zone is subjected to locally SW-migrating waves and a SW-directed sediment transport is produced (Longhitano & Colella, 2007). Many studies on the wave regime of the

Ionian Sea revealed that a strong seasonal oscillation of the wave amplitudes predominantly characterized this coastal tract, and the highest wave amplitudes are recorded during winter months, as December and January, and lowest during the period between June and August; indeed, the hydrodynamic conditions are of low or moderate energy and storm with wave height higher than 5 m are very rare (Ganea et al., 2017; Ghionis et al., 2015; Moschella et al., 2020).

3. METHODS

3.1 Dataset and shorelines extraction

The shorelines dataset included Landsat and Sentinel-2 imageries from 1972 to 2021 (**Fig. 3**), with a 10–year interval guaranteed to estimate the shoreline change rates. Only satellite images with a cloud cover percentage below 20% were used (Nassar et al., 2019; Quang et al., 2021a). The Landsat image bands selected are band 6/Short Wave Infrared 1 (SWIR 1) and band 3 (Green). In Sentinel-2 band 11 as SWIR and band 3 as Green were adopted. In 1991, 2001, and 2011 Landsat images, the Normalized Difference Water Index (NDWI) method was implemented because the Landsat images we used are of band 4 (NIR) and band 2 (green) on Landsat 4-5 TM and Landsat 7 ETM+. We employed band 5 (NIR) and band 3 (Green) of Landsat 8-9 OLI/TIRS in the NDWI analysis. The modified Normalized Difference Water Index (mNDWI), the Normalized Difference Water Index (NDWI), and the Normalized Difference Vegetation Index (NDVI) were employed to extract shoreline from each satellite image. All these indexes undertake a stable performance in distinguishing between water bodies and land and reducing built-up land noises (Xu, 2006; Feyisa et al., 2014; Fisher et al., 2016). Water pixel values were prescribed using a positive threshold in order to classify water bodies and land boundaries. The optimum threshold was 0 for all land–water classes (Xu & Gong, 2018; Cao et al., 2020). An annual coastline was created from the calculated Water Frequency Index (WFI) to identify shoreline changes. The formula for the WFI can be found in equation **1**.

$$\text{WFI} = \frac{\mathrm{N_{water}}}{\mathrm{N_{water}}+\mathrm{N_{land}}} \tag{1}$$

The symbols $\mathrm{N_{water}}$ and $\mathrm{N_{land}}$ were the number of pixels classified as water body and land within each year (Fisher et al., 2016; Xu, 2018). This method reduced the impact of sea-level changes on short-term and seasonal changes in sediment supply (Quang et al., 2021b; Xu, 2018). Water bodies and land in the 1972 and 1981 Landsat images were distinguished by adopting the Normalized Difference Vegetation Index (NDVI) method. In the NDVI method, the Landsat 1-3 images selected are band 6 (NIR) and 5 (red). In Landsat 4-5, we retrieved band 3 (NIR 1) and band 2 (Red). The formulas used for each of the mNDWI, NDWI, and NDVI methods can be seen in equations 2, 3, and 4 below (Chen et al., 2020; Liu et al., 2021):

$$\text{MNDWI} = \frac{(\text{Green} - \text{SWIR 1})}{(\text{Green} + \text{SWIR 1})} \quad (2)$$

$$\text{NDWI}= \frac{(\text{Green-NIR})}{(\text{Green+NIR})} \quad (3)$$

$$\text{NDVI} = \frac{(\text{NIR-Red})}{(\text{NIR + Red})} \quad (4)$$

Where:
MNDWI : the modified normalized difference water index
Green : band 2 of Landsat 4-5 TM, Landsat 7 ETM+, and Sentinel-2 images; band 3 in Landsat 8-9 OLI/TIRS
SWIR 1 : band 6 of Landsat image and band 11 of Sentinel-2 image
NDWI : the normalized difference water index
NIR : band 4 of Landsat 4-5 TM and Landsat 7 ETM+, band 5 in Landsat 8-9 OLI/TIRS, band 6 in Landsat 1-3 MSS, and band 3 in Landsat 4-5 MSS
NDVI : the normalized difference vegetation index
Red : band 5 of Landsat image 1-3 and band 2 in Landsat 4-5 MSS

There were three classes for each mNDW, NDWI, and NDVI, namely 0 for land, 1 for water description, and no data demonstrating locations covered by clouds and shadows. There were two ranges of WFI values: WFI ≥ 0.5 illustrated the annual water level, and WFI<0.5 implied the annual land surface. A description of the characteristics of each Landsat and Sentinel-2 imagery can be seen in **Table 1**. A Sentinel-2 image has the highest number of bands and the most detailed resolution compared to Landsat imageries.

3.2 Shoreline change rates and Digital Shoreline Analysis System

The coastal fringe under study was split into two segments using the Magnisi Peninsula as feature edge (**Fig. 2**). Segment 1 extends from the Mt. Tauro Cape to Magnisi Peninsula, Segment 2 is from the Magnisi Peninsula to the St. Panagia Cape and includes the longer sandy coastal tract. Shoreline change rates computation was then applied only to sandy coastlines and the statistical elaboration was run through the Digital Shoreline Analysis System (DSAS) v5.0 integrated with ArcGIS 10.8.1. Shoreline shift was so assessed by using the Net Shoreline Movement (NSM; equation 5), the Shoreline Change Envelope (SCE; equation 6), and the Weighted Linear Regression (WLR; equation 7). For the rate-of-change statistics calculation, the DSAS tool requires to set an uncertainty value which should include both positional and measurement errors (Himmelstoss et al., 2021). In the present study, the uncertainty value related to each image was computed according to Manno et al. (2017) and Virdis et al.

(2012) (Table in Supplementary Materials). The DSAS transect spacing and confidence interval were set at 25 m and 95%, respectively (**Fig. 4**).

$$\mathrm{NSM} = \text{distance (m) between oldest and youngest shoreline} \tag{5}$$

$$\mathrm{SCE} = \text{greatest distance(m) between all shorelines} \tag{6}$$

$$w = 1/e^2 \tag{7}$$

Where:

w : the weight of the variance function in measurement uncertainty and

e : the shoreline uncertainty value.

3.3 Coefficient of Coastal Armouring

The Coefficient of Coastal Armouring (K) is an index used to assess the grade of artificial coast. The K index is computed as the ratio between the total length (*l*) of all emerged and visible submerged maritime structures (groins, moles, seawalls, revetments, breakwaters, etc.) and the entire length (L) of the coast under study (Aybulatov & Artyukhin, 1993). The level of coastal armouring is qualitatively expressed in four classes, “Minimal” at K = 0.0001–0.1, “Average” when K = 0.11–0.5, “Maximal” at K = 0.51–1.0 and “Extreme” if K > 1.0.

4. RESULTS

4.1 Augusta Bay Shoreline Evolution

The medium-term shoreline change analysis of Augusta Bay was run using six shorelines covering a 49-year time interval (1972-2021). The shoreline evolution analysis was performed through the DSAS application and rate-of-change statistics were computed for 180 transects. As such, 157 transects recorded shoreline landward migration with WLR<0 and only 23 registered shoreline seaward shift with WLR>0. The WLR index ranged between a maximum value of 0.4 m/year, detected in correspondence of the Marcellino River mouth within Segment 1, in correspondence of the long sandy beach, and a minimum value of -1.4 m/year, found at the northern part of the Segment 2. However, both segments experienced negative shoreline movements with an average WLR values of -0.34 m/year and -0.69 m/year found in Segment 1 and Segment 2, respectively. As shown by the mean WLR, Segment 1 experienced a slighter shoreline recession than Segment 2, and the area of Porto Xifonio Bay and the Marcellino River mouth showed mainly a stable or accretional tendency. Segment 2 experienced a high variability and significant coastal retreat (**Fig.**).

The Net Shoreline Movement (NSM) and the Shoreline Change Envelope (SCE) were used to assess the spatial variability along the coast and in correspondence of each transect. The NSM reflects the distance between the oldest (1972) and youngest (2021) shorelines, without accounting the real spatial shoreline movement. The SCE expressed the measure of the total change in shoreline movement considering all available shoreline positions. The comparison between the two indexes shows that the erosional phenomena seemed to be constant over time along most of the coastal area (**Fig. 6**). Indeed, the Porto Xifonio Bay experienced slight seaward shoreline shift between 1972 and 1991, but intensive erosional phenomena were instead detected between 1991 and 2021. Similar trend was found southward the Marcellino River mouth, where beach accretion occurred between 1972 and 1991, then shoreline faced retreats till 2021. Constant shoreline landward movements were detected in correspondence with Segment 2 beach, where erosional phenomena already occurred from 1972 to 1991, but the tendency significantly decreased, and negative shoreline shifts of small entities were detected between 1991 and 2021.

4.2 Artificial coastline vs Natural coastline

The K index of Augusta Bay showed a significant increase from 0.40 to 0.70 between 1972 and 2021 (**Table 2**). Within Segment 1, artificial coastal structures were significantly implemented over last decades and the coastal armouring index increased by about 10%, passing from 0.53 registered in 1972 to 0.60 recorded in 2021. As such, the Segment 1 K index falls within the "Maximal" class range.

Segment 2 has a lower grade of coastal armouring than Segment 1, and the K index ranged from 0.10 to 0.12 between 1972 and 2021, so varying from the Minimal to Average class. However, the highest K index increase was recorded within Segment 2, and about 20% of natural coasts were here replaced by coastal structures in 49 years (**Fig. 7**).

5. DISCUSSION

5.1 Augusta Bay under human and natural forcings

Since the early 1950s, Augusta Bay faced increasing human pressures once the oil refinery was set up within this area. The new need to get access to the oil industries gave life to the effective implementation of transport infrastructures and urbanization. The Augusta port became a large-scale industrial harbour, and many coastal interventions were carried on during the time between the 1960s and the 1970s (Argnani et al., 2012; De Martini et al., 2012; Lentini et al., 2019; Smedile et al., 2012; Zaniboni et al., 2019). As such, the statistical shoreline changes analysis reveals that the recession is constant over the last 50 years. Indeed, the NSM and SCE indices showed that about 90% of the coast under study faced erosion, and only 10% of the analysed transects recorded a stability trend or slight sediment deposition.

The local wave regime is predominantly characterized by low or moderate energy events and not significantly affect the shoreline displacements. Most of the erosional phenomena were instead found in the correspondence of the torrent deltas, which are sites quite sensitive to sediment budget changes (Amrouni et al., 2019; Molina et al., 2019; Rosskopf et al., 2018). One of the explanations for these negative shoreline displacements could be the increasing number of hydraulic works (i.e. dams, fluvial barrages, artificial embankments) insisting along the waterways of the drainage basins, which triggered a reduction in the amount of water discharge and sediment load in the estuary (Amore & Giuffrida, 1985; Longhitano & Colella, 2007). Indeed, Di Stefano et al. (2013) pointed out how the Simeto drainage basin (30 Km N of Augusta) was anthropogenically modified with hydraulic conditions changes resulting in significant negative shoreline shifts at the Catania coastal plain area. However, subsidence phenomena of significant entity were detected within the Augusta Bay, indeed an average rate of -2 mm/yr, determined a constant shoreline landward migration (Polcari et al., 2018). The subsidence phenomenon exacerbated by marine extreme events such as seasonal and major storms (Medicane Qendresa, Medicane Zorbas, and Medicane Ianos) in 2014, 2018, and 2020 resulted in erosional processes tending to be more dominant than accretionary (Scicchitano et al., 2021).

5.2 Artificial coasts impact and shoreline response

The high level of artificial coasts seems to be a pivotal factor in increasing the coastal vulnerability to natural hazards (Jana & Bhattacharya, 2013). The Coastal Armouring Index (K) analysis applied to the coastal fringe of Augusta Bay showed a high level of artificial coast within the entire area since 1972. However, the increasing emplacement of coastal works was not constant throughout the entire coast. Indeed, Segment 1, extending between the Mt. Tauro Cape and the Magnisi Peninsula, was highly armoured since the beginning of the 1970s and registered a slower increase of the K index, varying from K = 0.53 to K = 0.60. Instead, Segment-2 revealed a minimal coastal armoured level in 1972 (K = 0.10), but the coastal armouring K passed from the Minimal class to the Average one with a value of 0.12, registering a percentage increase of the 20%. Despite the lower level of armouring, Segment 2 experienced significant erosional phenomena over the time between 1972 and 2021, and more than 97% of the coast faced landward shift (Fig. 8 . Depositional phenomena were instead observed in correspondence with shore-normal coastal structures, as detected within Segment 2, where two small groins were placed. However, a few meters from the shore-normal structures erosional phenomena occurred and this trend is commonly detected within the Mediterranean coastal area (Anfuso et al., 2012, 2013; Molina et al., 2019).

However, the Augusta Bay sediment longshore drift and coastal sediment dynamic was highly modified by the increasing coastal armouring, as shown by the computation of the K coefficient, and water and sediment exchange with the open sea is guaranteed only by the two inlets (Salvagio et al., 2016).

The high level of artificial coasts seems to be a pivotal factor in increasing the coastal vulnerability to natural hazards (Jana & Bhattacharya, 2013). As such, the higher average erosion velocity results compared to accretion can generally be interpreted to mean that the negative correlation between shoreline curvature and longshore current, such as residential and industrial development, has a more significant influence than the construction of coastal structures to prevent coastal erosion. These insights should push administrations to wisely plan coastal land use, the watershed management and to adopt more environmental and ecological measures to better face coastal hazards. Indeed, recent research showed how nature-based solutions are valuable, effective and low-cost works to prevent or reduce coastal erosion risk (Duarte et al., 2013; Gracia et al., 2018; O'Leary et al., 2023). When possible, restoring dune systems vegetation or submerged seafloor vegetation (i.e. *Posidonia* seagrasses) is demonstrated to be a winning strategy in counteracting the increasing human and natural pressing on coastal ecosystems, especially in light of future sea-level rise scenarios (Fernández-Montblanc et al., 2020; Van Rooijen et al., 2016; Vuik et al., 2016). For these reasons, a more detailed study regarding the influence of marine natural hazards and human activities on coastline changes in the east of Sicily also requires to be carried out to determine the right solution in anticipating the worst events that can cause casualties and economic losses. These study results are the first step in revealing shoreline changes with a more comprehensive and detailed method. In the future, the implication simulation of tsunamis, storms, sediment supply, sea–level changes, and human activities on shoreline changes is essential to be conducted.

5. CONCLUSIONS

The Augusta Bay is a coastal densely populated area playing an economic key-role within Italy. The shoreline evolution of Augusta Bay was investigated over the time between 1972 and 2021. The analysis showed that most of the coast faced severe landward migration and significant coastal armoring was recorded since the 1970s. Within Segment 1 (Mt. Tauro Cape-Magnisi Peninsula) shoreline changes are dominated by erosion with an average rate of −0.34 m/year. Segment 2 (Magnisi Peninsula-St. Panagia Cape) has a higher erosion rate than Segment 1 with a value of −0.69 m/year. The coastal strip is highly armoured, and the coastal armouring of Segment 1 is Maximal and any significant changes emerged from the analysis. Segment 2 coastal armouring index passed from the Minimal class to the Average one with a percentage increase of 20%. What emerged so far is that Augusta Bay is experiencing significant retreating;

on one hand, the low riverine sediment load, the significant subsidance rate and the longshore drift led the shoreline moving landward, while the high level of artificial coast altered the sediment transport and affect the local coastal dynamic. However, this research is the first step in the comprehension of the evolution of Augusta Bay, a strategic infrastructural area within Southern Sicily, but further research is needed to better understand the drainage basin regime and the coastal human pressure on the littoral changes of this coastal strip.

REFERENCES

Aladwani, N. S. (2022). Shoreline change rate dynamics analysis and prediction of future positions using satellite imagery for the southern coast of Kuwait: A case study. Oceanologia, 64, 417-432. https://doi.org/10.1016/J.OCEANO.2022.02.002

Amore, C., & Giuffrida, E. (1985). L'influenza dell'interrimento dei bacini artificiali del F. Simeto sul litorale del Golfo di Catania. Bollettino della Società geologica italiana, 103, 731–753.

Amrouni, O., Hzami, A., & Heggy, E. (2019). Photogrammetric assessment of shoreline retreat in North Africa: Anthropogenic and natural drivers. ISPRS Journal of Photogrammetry and Remote Sensing, 157, 73-92. https://doi.org/10.1016/j.isprsjprs.2019.09.001

Anfuso, G., Martínez-del-Pozo, J. Á., & Rangel-Buitrago, N. (2012). Bad practice in erosion management: the southern Sicily case study. In: Cooper, J., Pilkey, O. (ed) Pitfalls of shoreline stabilization. Springer, Netherlands, 215-233. https://doi.org/10.1007/978-94-007-4123-2_13

Anfuso, G., Martínez-del-Pozo, J. Á., & Rangel-Buitrago, N. (2013). Morphological cells in the Ragusa littoral (Sicily, Italy). Journal of Coastal Conservation, 17(3), 369–377. https://doi.org/10.1007/s11852-013-0233-8

Argnani, A., Armigliato, A., Pagnoni, G., Zaniboni, F., Tinti, S., & Bonazzi, C. (2012). Active tectonics along the submarine slope of south-eastern Sicily and the source of the 11 January 1693 earthquake and tsunami. Natural Hazards and Earth System Sciences, 12(5), 1311-1319. https://doi.org/10.5194/nhess-12-1311-2012

Aybulatov, N. A., & Artyukhin, Y. V. (1993). Geo-ecology of the world ocean`s shelf and coasts. Hydrometeo Publishing.

Bacino, G. L., Dragani, W. C., Codignotto, J. O., Pescio, A. E., & Farenga, M. O. (2020). Shoreline change rates along Samborombón Bay, Río de la Plata estuary, Argentina. Estuarine, Coastal and Shelf Science, 237, 106659. https://doi.org/10.1016/j.ecss.2020.106659

Ben-Avraham, Z., & Grasso, M. (1991). Crustal structure variations and transcurrent faulting at the eastern and western margins of the eastern Mediterranean. Tectonophysics, 196(3-4), 269-277. https://doi.org/10.1016/0040-1951(91)90326-N

Ben-Avraham, Z., & Ginzburg, A. (1990). Displaced terranes and crustal evolution of the Levant and the eastern Mediterranean. Tectonics, 9(4), 613-622. https://doi.org/10.1029/TC009i004p00613

Bianca, M., Monaco, C., Tortorici, L., & Cernobori, L. (1999). Quaternary normal faulting in southeastern Sicily (Italy): A seismic source for the 1693 large earthquake. Geophysical Journal International, 139(2), 370-394. https://doi.org/10.1046/j.1365-246X.1999.00942.x

Borzì, L., Anfuso, G., Manno, G., Distefano, S., Urso, S., Chiarella, D., & Di Stefano, A. (2021). Shoreline evolution and environmental changes at the nw area of the gulf of gela (Sicily, italy). Land, 10(10), 1034. https://doi.org/10.3390/land10101034

Burollet, P. F., Mugniot, J. M., & Sweeney, P. (1978). The Geology of the Pelagian Block: The Margins and Basins off Southern Tunisia and Tripolitania. The ocean basins and margins (pp. 331-359). https://doi.org/10.1007/978-1-4684-3039-4_6

Cai, F., Su, X., Liu, J., Li, B., & Lei, G. (2009). Coastal erosion in China under the condition of global climate change and measures for its prevention. Progress in Natural Science, 19(4), 415-426. https://doi.org/10.1016/j.pnsc.2008.05.034

Cao, W., Zhou, Y., Li, R., & Li, X. (2020). Mapping changes in coastlines and tidal flats in developing islands using the full time series of Landsat images. Remote Sensing of Environment, 239, 111665. https://doi.org/10.1016/j.rse.2020.111665

Carbone, S., Barbano, M. S., Cantarella, G. L., Ferrara, G., Lentini, F., Longhitano, S., Maniscalco, R., Marino, M., Martino, C., Ruggeri, R., Scribano, V., Tiralongo, P., & Zanini, A. (2011). Carta Geologica d'Italia alla scala 1:50000 (Progetto CARG): Foglio 641 Augusta e Note Illustrative. El. Ca. Florence, 641, 1-247.

Carbone, S., Di Geronimo, I., Grasso, M., Iozzia, S., & Lentini, F. (1982). I terrazzi marini quaternari dell’area iblea. Contr. alia realizz, della Carta Neotettonica d’ltalia. In Giannini (Eds.) Geodinamica (506), Napoli.

Carbone, S., Grasso, M., Lentini, F., Lombardo, G., & Patane, G. (1987). Lineamenti geologici del plateau Ibleo (Sicilia SE). Presentazione delle carte geologiche della Sicilia Sud-Orientale. Memoir Society Geology Italy, 38(1), 127–135.

Catalano, S., Romagnoli, G., & Tortorici, G. (2010). Kinematics and dynamics of the Late Quaternary rift-flank deformation in the Hyblean Plateau (SE Sicily). Tectonophysics, 486(1-4), 1-14. https://doi.org/10.1016/j.tecto.2010.01.013

Chen, F., Chen, X., Van de Voorde, T., Roberts, D., Jiang, H., & Xu, W. (2020). Open water detection in urban environments using high spatial resolution remote sensing imagery. Remote Sensing of Environment, 242, 111706. https://doi.org/10.1016/j.rse.2020.111706

Chu, L., Oloo, F., Sudmanns, M., Tiede, D., Hölbling, D., Blaschke, T., & Teleoaca, I. (2020). Monitoring long-term shoreline dynamics and human activities in the Hangzhou Bay, China, combining daytime and nighttime EO data. Big Earth Data, 4(3), 242-264. https://doi.org/10.1080/20964471.2020.1740491

De Martini, P. M., Barbano, M. S., Pantosti, D., Smedile, A., Pirrotta, C., Del

Carlo, P., & Pinzi, S. (2012). Geological evidence for paleotsunamis along eastern Sicily (Italy): An overview. Natural Hazards and Earth System Sciences, 12(8), 2569-2580. https://doi.org/10.5194/nhess-12-2569-2012

Di Stefano, A., De Pietro, R., Monaco, C., & Zanini, A. (2013). Anthropogenic influence on coastal evolution: A case history from the Catania Gulf shoreline (eastern Sicily, Italy). Ocean and Coastal Management, 80, 133-148. https://doi.org/10.1016/j.ocecoaman.2013.02.013

Distefano, S., & Gamberi, F. (2022). Preservation of Transgressive System Tract Geomorphic Elements during the Holocene Sea Level Rise in the South-Eastern Sicilian Tyrrhenian Margin. Journal of Marine Science and Engineering, 10(8), 1013. https://doi.org/10.3390/jmse10081013

Distefano, S., Gamberi, F., Baldassini, N., & Di Stefano, A. (2019a). Neogene stratigraphic evolution of a tectonically controlled continental shelf: The example of the Lampedusa island. Italian Journal of Geosciences, 138, 418-431. https://doi.org/10.3301/IJG.2019.17

Distefano, S., Gamberi, F., Baldassini, N., & Di Stefano, A. (2021a). Quaternary evolution of coastal plain in response to sea-level changes: Example from south-east sicily (southern italy). Water (Switzerland), 13(11), 1524. https://doi.org/10.3390/w13111524

Distefano, S., Gamberi, F., Baldassini, N., & Stefano, A. D. I. (2018). Late Miocene to quaternary structural evolution of the Lampedusa island offshore. Geografia Fisica e Dinamica Quaternaria, 41(2), 17-31. https://doi.org/10.4461/GFDQ.2018.41.10

Distefano, S., Gamberi, F., Borzì, L., & Di Stefano, A. (2021b). Quaternary coastal landscape evolution and sea-level rise: An example from south-east sicily. Geosciences (Switzerland), 11(12), 506. https://doi.org/10.3390/geosciences11120506

Distefano, S., Gamberi, F., & Di Stefano, A. (2019b). Stratigraphic and structural reconstruction of an offshore sector of the Hyblean Foreland ramp (southern Italy). Italian Journal of Geosciences, 138, 390-403. https://doi.org/10.3301/IJG.2019.12

Duarte, C. M., Losada, I. J., Hendriks, I. E., Mazarrasa, I., & Marbà, N. (2013). The role of coastal plant communities for climate change mitigation and adaptation. Nature Climate Change, 3(11), 961–968. https://doi.org/10.1038/nclimate1970

Fernández-Montblanc, T., Duo, E., & Ciavola, P. (2020). Dune reconstruction and revegetation as a potential measure to decrease coastal erosion and flooding under extreme storm conditions. Ocean & Coastal Management, 188, 105075. https://doi.org/https://doi.org/10.1016/j.ocecoaman.2019.105075

Feyisa, G. L., Meilby, H., Fensholt, R., & Proud, S. R. (2014). Automated Water Extraction Index: A new technique for surface water mapping using Landsat imagery. Remote Sensing of Environment, 140, 23-35. https://doi.org/10.1016/j.rse.2013.08.029

Firetto, C. M., Di Stefano, A., & Budillon, F. (2013). Seismic facies and seabed morphology in a tectonically controlled continental shelf: The Augusta Bay (offshore eastern Sicily, Ionian Sea). Marine Geology, 335, 35-51. https://doi.org/10.1016/j.margeo.2012.10.009

Fisher, A., Flood, N., & Danaher, T. (2016). Comparing Landsat water index methods for automated water classification in eastern Australia. Remote Sensing of Environment, 175, 167-182. https://doi.org/10.1016/j.rse.2015.12.055

Fletcher, C. H., Romine, B. M., Genz, A. S., Barbee, M. M., Dyer, M., Anderson, T. R., Lim, S. C., Vitousek, S., Bochicchio, C., & Richmond, B. M. (2012). National assessment of shoreline change; historical shoreline change in the Hawaiian Islands. U.S. Geological Survey Open-File Report 2011-1051. Retrieved February 19, 2022, from http://pubs.usgs.gov/of/2011/1051

Gamberi, F., Della Valle, G., Marani, M., Mercorella, A., Distefano, S., & Di Stefano, A. (2019). Tectonic controls on sedimentary system along the continental slope of the central and southeastern Tyrrhenian Sea. Italian Journal of Geosciences, 138(3), 317-332. https://doi.org/10.3301/IJG.2019.08

Ganea, D., Amortila, V., Mereuta, E., & Rusu, E. (2017). A joint evaluation of the wind and wave energy resources close to the Greek Islands. Sustainability (Switzerland), 9(6), 1025. https://doi.org/10.3390/su9061025

Ghionis, G., Poulos, S. E., Verykiou, E., Karditsa, A., Alexandrakis, G., & Andris, P. (2015). The impact of an extreme storm event on the barrier beach of the Lefkada lagoon, NE Ionian Sea (Greece). Mediterranean Marine Science, 16(3), 562-572. https://doi.org/10.12681/mms.948

Gracia, A., Rangel-Buitrago, N., Oakley, J. A., & Williams, A. T. (2018). Use of ecosystems in coastal erosion management. Ocean & Coastal Management, 156, 277–289. https://doi.org/https://doi.org/10.1016/j.ocecoaman.2017.07.009

Himmelstoss, E. A., Henderson, R. E., Kratzmann, M. G., & Farris, A. S. (2021). Digital Shoreline Analysis System (DSAS) version 5.1 user guide. U.S. Geological Survey Open-File Report 2021-1091. Retrieved May 18, 2023, from https://doi.org/10.3133/ofr20211091

Holman, R., Sallenger, A., Lippmann, T., & Haines, J. (1993). The application of video image processing to the study of nearshore processes. Oceanography, 6(3), 78–85. https://doi.org/10.5670/oceanog.1993.02

Jana, A., & Bhattacharya, A. K. (2013). Assessment of coastal erosion vulnerability around Midnapur-Balasore Coast, Eastern India using integrated remote sensing and GIS techniques. Journal of the Indian Society of Remote Sensing, 41(3), 675-686. https://doi.org/10.1007/s12524-012-0251-2

Johnston, W. G., Cooper, J. A. G., & Olynik, J. (2023). Shoreline change on a tropical island beach, Seven Mile Beach, Grand Cayman: The influence of beachrock and shore protection structures. Marine Geology, 457, 107006.

https://doi.org/https://doi.org/10.1016/j.margeo.2023.107006

Laksono, F. A. T., Borzì, L., Distefano, S., Di Stefano, A., & Kovács, J. (2022b). Shoreline prediction modelling as a base tool for coastal management: The Catania Plain case study (Italy). Journal of Marine Science and Engineering, 10(12), 1988. https://doi.org/10.3390/jmse10121988

Laksono, F. A. T., Widagdo, A., Aditama, M. R., Fauzan, M. R., & Kovács, J. (2022a). Tsunami Hazard Zone and Multiple Scenarios of Tsunami Evacuation Route at Jetis Beach, Cilacap Regency, Indonesia. Sustainability (Switzerland), 14(5), 2726. https://doi.org/10.3390/su14052726

Lentini, V., Castelli, F., & Lombardo, C. (2019). Seismic risk evaluation for refineries: The case of Augusta petrochemical area (Sicily, Italy). In: Silvestri, F., & Moraci, N. (ed) Earthquake geotechnical engineering for protection and development of environment and constructions. CRC Press, Rome, 8. https://doi.org/10.1201/9780429031274

Lippmann, T. C., & Holman, R. A. (1989). Quantification of sand bar morphology: a video technique based on wave dissipation. Journal of Geophysical Research, 94(C1), 995-1011. https://doi.org/10.1029/JC094iC01p00995

Liu, Q., Liu, L., Zhang, Y., Wang, Z., Wu, J., Li, L., Li, S., & Paudel, B. (2021). Identification of impact factors for differentiated patterns of NDVI change in the headwater source region of Brahmaputra and Indus, Southwestern Tibetan Plateau. Ecological Indicators, 125, 107604. https://doi.org/10.1016/j.ecolind.2021.107604

Longhitano, S., & Colella, A. (2007). Geomorphology, sedimentology and recent evolution of the anthropogenically modified Simeto River delta system (eastern Sicily, Italy). Sedimentary Geology, 194(3–4), 195-221. https://doi.org/10.1016/j.sedgeo.2006.06.004

Maniscalco, R., Fazio, E., Punturo, R., Cirrincione, R., Di Stefano, A., Distefano, S., Forzese, M., Lanzafame, G., Leonardi, G. S., Montalbano, S., Pellegrino, A. G., Raele, A., & Palmeri, G. (2022). The porosity in heterogeneous carbonate reservoir rocks: tectonic versus diagenetic imprint—A multi-scale study from the Hyblean Plateau (SE Sicily, Italy). Geosciences (Switzerland), 12(4), 149. https://doi.org/10.3390/geosciences12040149

Manno, G., Lo Re, C., & Ciraolo, G. (2017). Uncertainties in shoreline position analysis: The role of run-up and tide in a gentle slope beach. Ocean Science, 13(5), 661-671. https://doi.org/10.5194/os-13-661-2017

Margheriti, L. (2021). Seismic surveillance and earthquake monitoring in Italy. Seismological Research Letters, 92(3), 1659-1671. https://doi.org/10.1785/0220200380

Molina, R., Anfuso, G., Manno, G., & Prieto, F. J. G. (2019). The Mediterranean coast of Andalusia (Spain): Medium-term evolution and impacts of coastal structures. Sustainability (Switzerland), 11(13), 3539. https://doi.org/10.3390/su11133539

Moschella, S., Cannata, A., Cannavò, F., Di Grazia, G., Nardone, G., Orasi, A., Picone, M., Ferla, M., & Gresta, S. (2020). Insights into microseism sources by array and machine learning techniques: Ionian and Tyrrhenian Sea case of study. Frontiers in Earth Science, 8, 114. https://doi.org/10.3389/feart.2020.00114

Nassar, K., Mahmod, W. E., Fath, H., Masria, A., Nadaoka, K., & Negm, A. (2019). Shoreline change detection using DSAS technique: Case of North Sinai coast, Egypt. Marine Georesources and Geotechnology, 37(1), 81-95. https://doi.org/10.1080/1064119X.2018.1448912

O'Leary, B. C., Fonseca, C., Cornet, C. C., de Vries, M. B., Degia, A. K., Failler, P., Furlan, E., Garrabou, J., Gil, A., Hawkins, J. P., Krause-Jensen, D., Le Roux, X., Peck, M. A., Pérez, G., Queirós, A. M., Różyński, G., Sanchez-Arcilla, A., Simide, R., Sousa, P.I., Roberts, C. M. (2023). Embracing Nature-based Solutions to promote resilient marine and coastal ecosystems. Nature-Based Solutions, 3, 100044. https://doi.org/https://doi.org/10.1016/j.nbsj.2022.100044

Pirrotta, C., Barbano, M. S., Pantosti, D., & De Martini, P. M. (2013). Evidence of active tectonics in the Augusta Basin (eastern Sicily, Italy) by Chirp sub-bottom sonar investigation. Annals of Geophysics, 56(5), S0562. https://doi.org/10.4401/ag-6371

Plant, N. G., & Holman, R. A. (1997). Intertidal beach profile estimation using video images. Marine Geology, 140(1–2), 1–24. https://doi.org/10.1016/S0025-3227(97)00019-4

Polcari, M., Albano, M., Montuori, A., Bignami, C., Tolomei, C., Pezzo, G., Falcone, S., Piana, C. La, Doumaz, F., Salvi, S., & Stramondo, S. (2018). InSAR monitoring of Italian coastline revealing natural and anthropogenic ground deformation phenomena and future perspectives. Sustainability (Switzerland), 10(9), 3152. https://doi.org/10.3390/su10093152

Quang, D. N., Linh, N. K., Tam, H. S., & Viet, N. T. (2021a). Remote sensing applications for reservoir water level monitoring, sustainable water surface management, and environmental risks in Quang Nam province, Vietnam. Journal of Water and Climate Change, 12(7), 3045-3063. https://doi.org/10.2166/wcc.2021.347

Quang, D. N., Ngan, V. H., Tam, H. S., Viet, N. T., Tinh, N. X., & Tanaka, H. (2021b). Long-term shoreline evolution using dsas technique: A case study of Quang Nam province, Vietnam. Journal of Marine Science and Engineering, 9(10), 1124. https://doi.org/10.3390/jmse9101124

Rezaee, M., Golshani, A., & Mousavizadegan, H. (2019). A new methodology to analysis and predict shoreline changes due to human interventions (case study: Javad Al-Aemmeh port, Iran). International Journal of Maritime Technology, 12, 9–23. https://doi.org/10.29252/ijmt.12.9

Rosskopf, C. M., Di Paola, G., Atkinson, D. E., Rodríguez, G., & Walker, I. J. (2018). Recent shoreline evolution and beach erosion along the central Adriatic coast of Italy: the case of Molise region. Journal of Coastal Conservation, 22(5), 879-895.

https://doi.org/10.1007/s11852-017-0550-4

Salvagio, M.D., Bonsignore, M., Elvira, O., Barra, M., Tranchida, G., Giaramita, L., Mazzola, S., & Sprovieri, M. (2016). Fluxes and the mass balance of mercury in Augusta Bay (Sicily, southern Italy). Estuarine, Coastal and Shelf Science, 181, 134-143. https://doi.org/10.1016/j.ecss.2016.08.013

Santos, C. A. G., Nascimento, T. V. M., Mishra, M., & Silva, R. M. (2021). Analysis of long- and short-term shoreline change dynamics: A study case of João Pessoa city in Brazil. Science of the Total Environment, 769, 144889. https://doi.org/10.1016/j.scitotenv.2020.144889

Scicchitano, G., Antonioli, F., Berlinghieri, E. F. C., Dutton, A., & Monaco, C. (2008). Submerged archaeological sites along the Ionian coast of southeastern Sicily (Italy) and implications for the Holocene relative sea-level change. Quaternary Research, 70(1), 26-39. https://doi.org/10.1016/j.yqres.2008.03.008

Scicchitano, G., & Monaco, C. (2006). Grotte carsiche e linee di costa sommerse tra Capo Santa Panagia e Ognina (Siracusa, Sicilia sud-orientale). Alpine and Mediterranean Quaternary, 19(2), 187–194.

Scicchitano, G., Scardino, G., Monaco, C., Piscitelli, A., Milella, M., De Giosa, F., & Mastronuzzi, G. (2021). Comparing impact effects of common storms and Medicanes along the coast of south-eastern Sicily. Marine Geology, 439, 106556. https://doi.org/10.1016/j.margeo.2021.106556

Selvaggi, R., Pappalardo, G., Chinnici, G., & Fabbri, C. I. (2018). Assessing land efficiency of biomethane industry: A case study of Sicily. Energy Policy, 119, 689–695. https://doi.org/10.1016/j.enpol.2018.04.039

Smedile, A., De Martini, P. M., & Pantosti, D. (2012). Combining inland and offshore paleotsunamis evidence: The Augusta Bay (eastern Sicily, Italy) case study. Natural Hazards and Earth System Science, 12(8), 2557-2567. https://doi.org/10.5194/nhess-12-2557-2012

Spampinato, C. R., Costa, B., Di Stefano, A., Monaco, C., & Scicchitano, G. (2011). The contribution of tectonics to relative sea-level change during the Holocene in coastal south-eastern Sicily: New data from boreholes. Quaternary International, 232(1–2), 214-227. https://doi.org/10.1016/j.quaint.2010.06.025

Sprovieri, M., Oliveri, E., Di Leonardo, R., Romano, E., Ausili, A., Gabellini, M., Barra, M., Tranchida, G., Bellanca, A., Neri, R., Budillon, F., Saggiomo, R., Mazzola, S., & Saggiomo, V. (2011). The key role played by the Augusta basin (southern Italy) in the mercury contamination of the Mediterranean Sea. Journal of Environmental Monitoring, 13(6), 1753-1760. https://doi.org/10.1039/c0em00793e

Todd, P. A., Heery, E. C., Loke, L. H. L., Thurstan, R. H., Kotze, D. J., & Swan, C. (2019). Towards an urban marine ecology: characterizing the drivers, patterns and processes of marine ecosystems in coastal cities. Oikos, 128(9), 1215-1242. https://doi.org/10.1111/oik.05946

Van Rooijen, A. A., McCall, R. T., Van Thiel de Vries, J. S. M., Van Dongeren, A. R., Reniers, A. J. H. M., & Roelvink, J. A. (2016). Modeling the effect of wave-vegetation interaction on wave setup. Journal of Geophysical Research: Oceans, 121(6), 4341-4359. https://doi.org/10.1002/2015JC011392

Virdis, S. G. P., Oggiano, G., & Disperati, L. (2012). A geomatics approach to multitemporal shoreline analysis in western mediterranean: The case of platamona-maritza beach (Northwest Sardinia, Italy). Journal of Coastal Research, 28(3), 624-640. https://doi.org/10.2112/JCOASTRES-D-11-00078.1

Vuik, V., Jonkman, S. N., Borsje, B. W., & Suzuki, T. (2016). Nature-based flood protection: The efficiency of vegetated foreshores for reducing wave loads on coastal dikes. Coastal Engineering, 116, 42–56. https://doi.org/https://doi.org/10.1016/j.coastaleng.2016.06.001

Wang, X., Yan, F., & Su, F. (2021). Changes in coastline and coastal reclamation in the three most developed areas of China, 1980–2018. Ocean & Coastal Management, 204, 105542. https://doi.org/10.1016/J.OCECOAMAN.2021.105542

Xu, H. (2006). Modification of normalised difference water index (NDWI) to enhance open water features in remotely sensed imagery. International Journal of Remote Sensing, 27(14), 3025-3033. https://doi.org/10.1080/01431160600589179

Xu, N. (2018). Detecting coastline change with all available landsat data over 1986-2015: A case study for the state of Texas, USA. Atmosphere, 9(3), 107. https://doi.org/10.3390/atmos9030107

Xu, N., & Gong, P. (2018). Significant coastline changes in China during 1991–2015 tracked by Landsat data. Science Bulletin, 63(14), 883–886. https://doi.org/10.1016/J.SCIB.2018.05.032

Zaniboni, F., Pagnoni, G., Gallotti, G., Ausilia P.M., Armigliato, A., & Tinti, S. (2019). Assessment of the 1783 Scilla landslide-tsunami's effects on the Calabrian and Sicilian coasts through numerical modeling. Natural Hazards and Earth System Sciences, 19(8), 1585-1600. https://doi.org/10.5194/nhess-19-1585-2019

Zhang, Y., Wang, G., Li, Q., Huang, W., Liu, X., Chen, C., Shi, X., & Zheng, J. (2021). Vulnerability assessment of nearshore clam habitat subject to storm waves and surge. Scientific Reports, 11(1), 569. https://doi.org/10.1038/s41598-020-80863-4

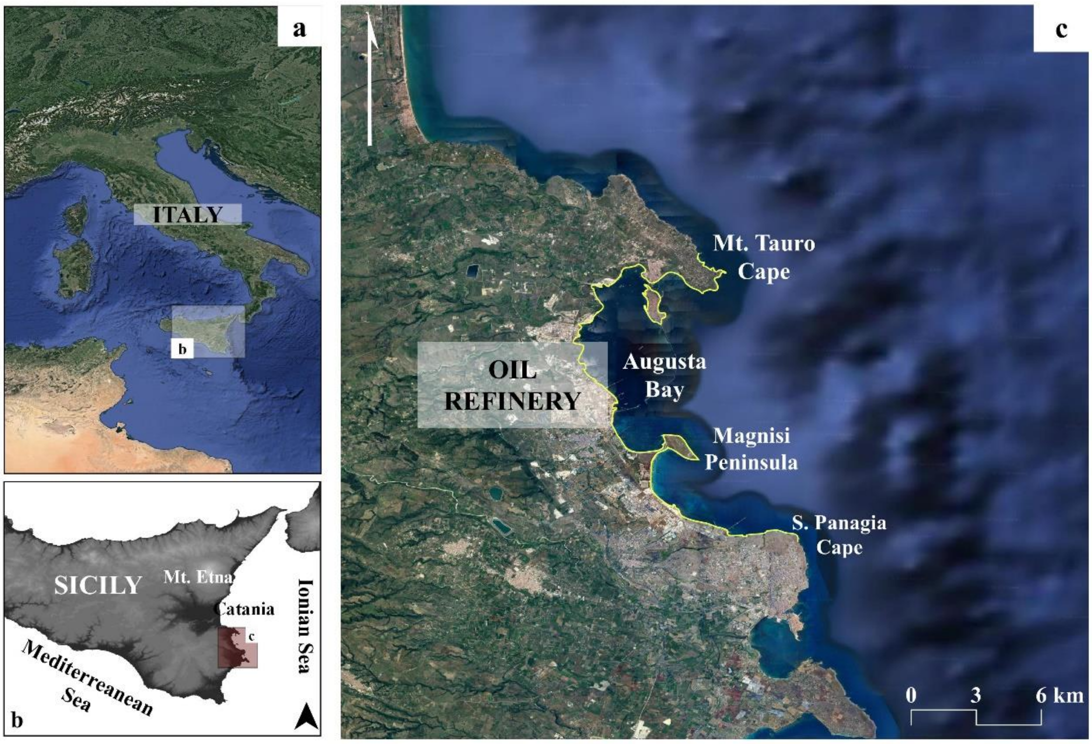

Fig. 1 - a) The study area is in Southern Italy and falls within the region of Sicily; **b)** the study area is southern the town of Catania, facing the Ionian Sea; **c)** the Augusta Bay coastal sector extended from the Mt. Tauro Cape to the Panagia Cape; the coastal area is split by the Magnisi Peninsula. The yellow line is the coastal tract studied in the present paper.

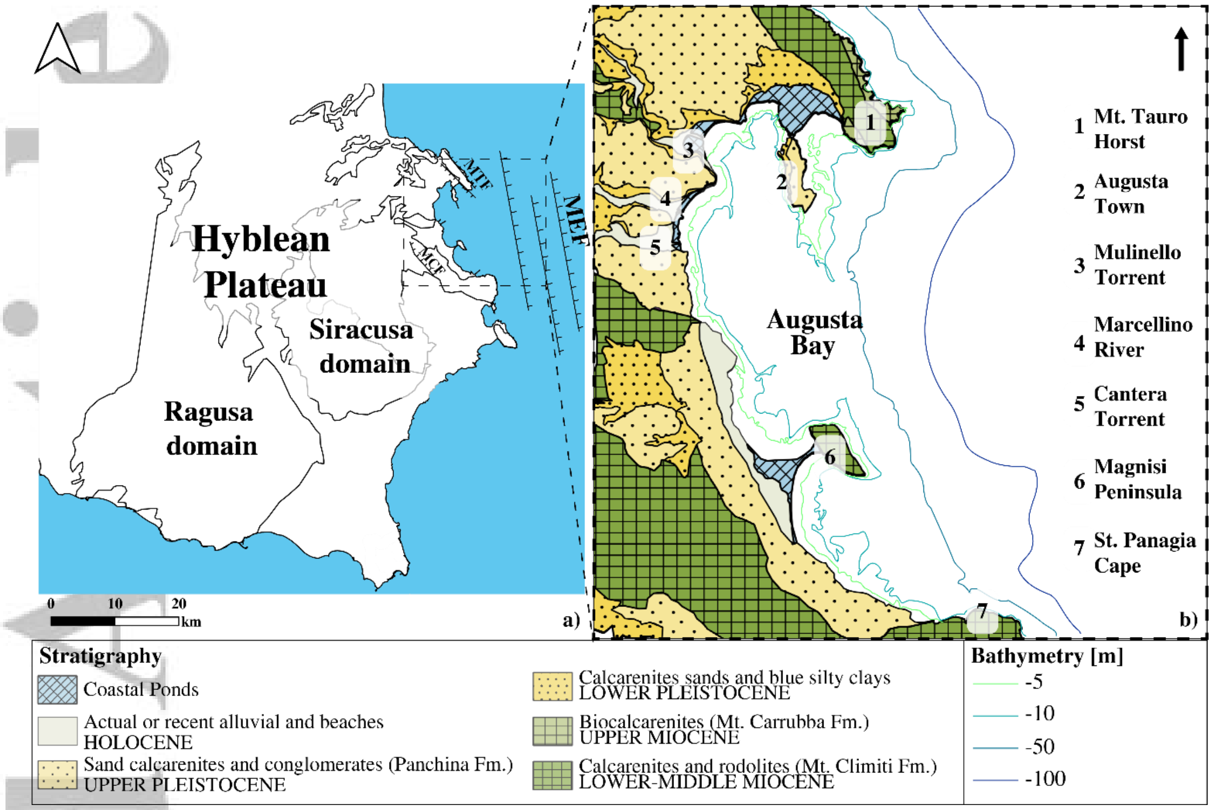

Fig. 2 - a) Structural and **b)** geological sketch-map of the Augusta Bay. The study area falls within the Eastern part of the Hyblean Plateau, where a Mesozoic-Cenozoic shallow-water to basin carbonate sedimentary succession outcrops. *MEF = Malta Escarpment Fault; MTF = Mt. Tauro Fault; MCF = Mt. Climiti Fault*.

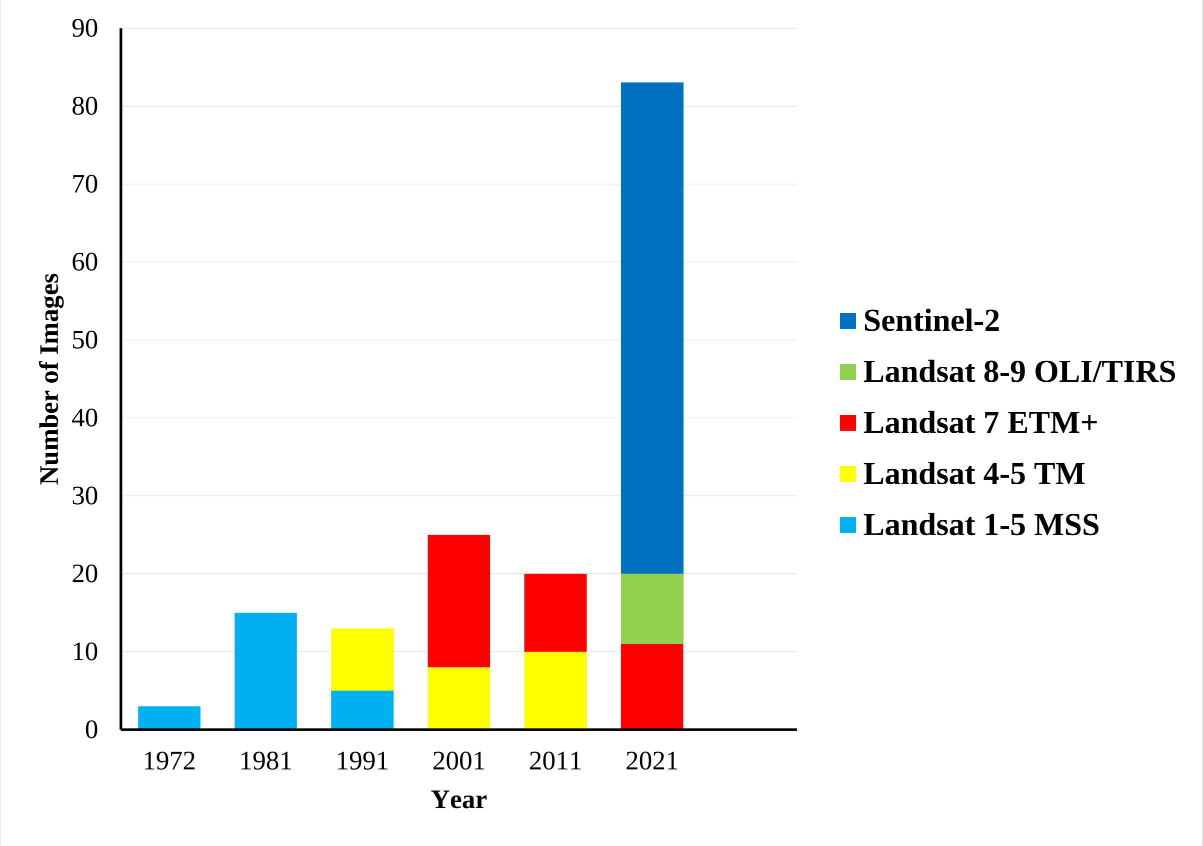

Fig. 3 The number of Landsat and Sentinel-2 image series from 1972 to 2021 was used in this study. For analysis of shoreline changes in 1972 and 1981, we used Landsat 1–5 MSS. Landsat 7 ETM+, Landsat 8 OLI/TIRS, and Sentinel–2 are applied for shoreline delineation in 2021.

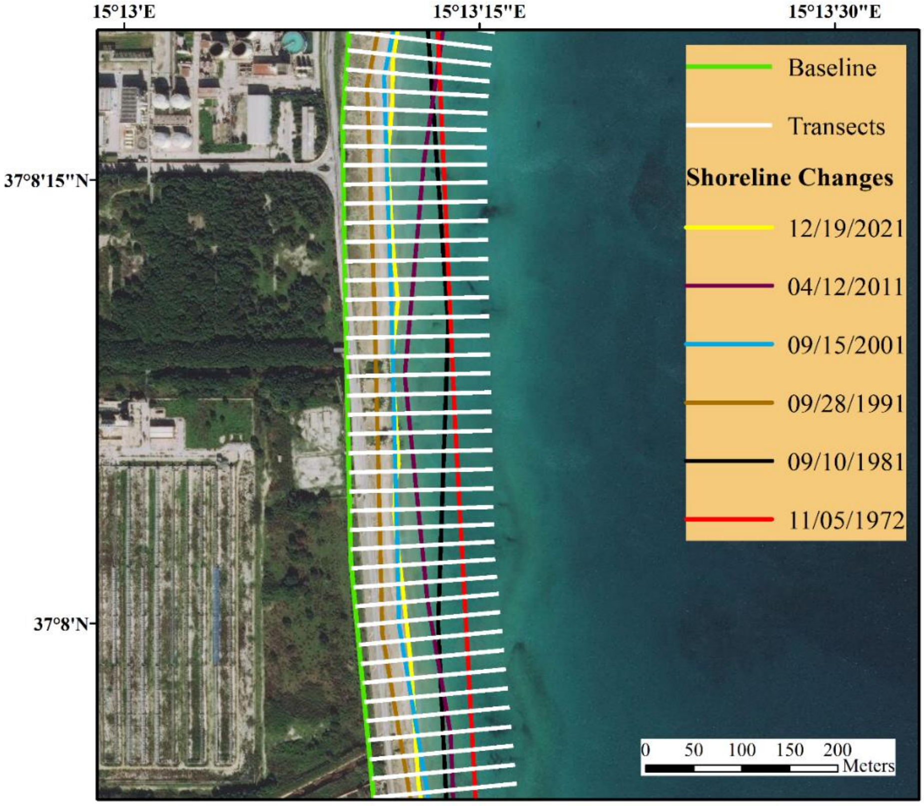

Fig. 4 Illustration of transect delineation for shoreline analysis in Augusta using DSAS 5.0. The transect spacing was 25 m. Basemap was acquired from U.S. Geological Survey.

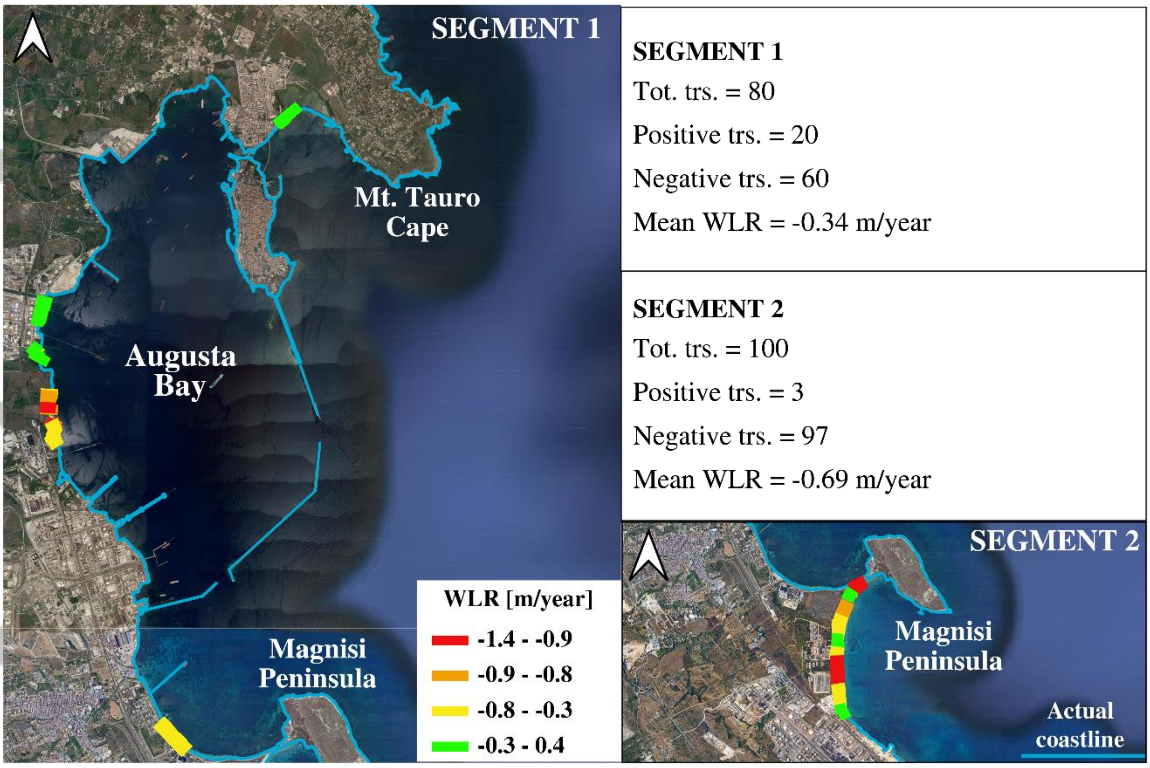

Fig. 5 The shoreline evolution of Augusta Bay. The shoreline shift is expressed as WLR and classes intervals were set according to natural breaks. Segment 1, which extends from the Mt. Tauro Cape to Magnisi Peninsula, experienced significant landward migration, up to -1.4 m/year, even though slower retreats were detected in correspondence with the Marcellino River mouth. Segment 2 corresponds with the longer coastal sandy beach tract and counts a higher number of transects that registered negative WLR values (97). *Trs = Transects; WLR = Weighted Linear Regression Rate.*

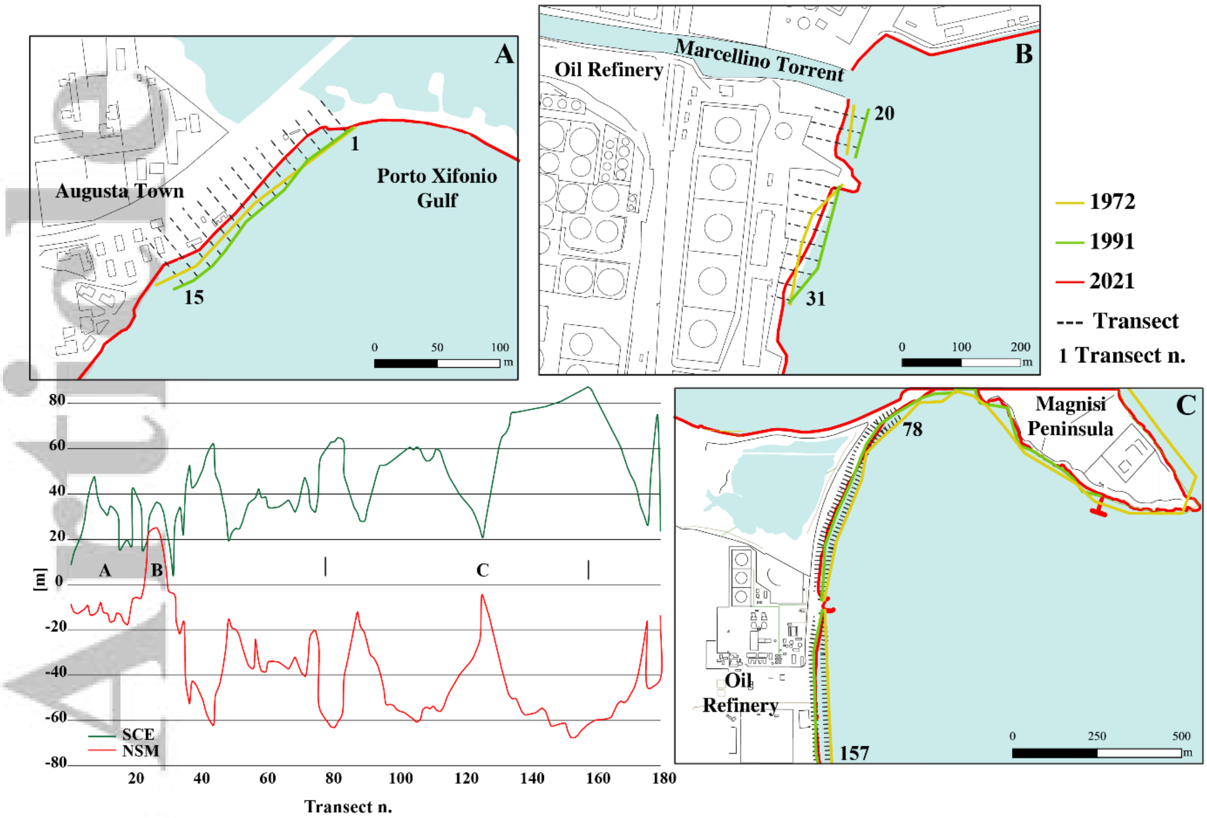

Fig. 6 The Net Shoreline Movement (NSM) and the Shoreline Change Envelope (SCE) plots. The shoreline evolution of Augusta Bay was mainly negative, but the NSM index showed that the shoreline migration was not constant over time.

Fig. 7 The coastal morphology types of Augusta Bay in 2021. Most of the coast is highly armoured.

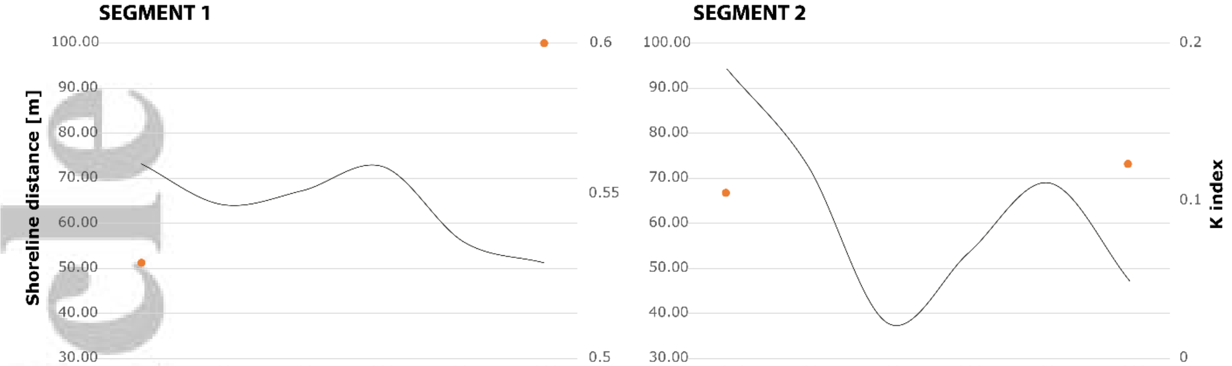

Fig. 8 Augusta Bay shoreline evolution coupled with Coastal Armouring Index (K). The black line represents the shoreline distance from the baseline registered for each year. The orange dot is the K index value obtained for the 1972 and the 2021.

Table 1 Characteristics of Landsat and Sentinel-2 images include sensor type, spatial resolution, number of bands, near-infrared (NIR), and repeat cycle (Cao et al., 2020; Quang et al., 2021a).

Satellite Image	Resolution (m)	Year	Sensors	Number of bands	Current Status	Green Band	NIR	Revisit Time (Days)
Landsat 1–5	60–80	1972, 1981, and 1991	MSS	4	Ended 1992	Band 4 for Landsat MSS 1-3 spectral bands. Band 1 for Landsat MSS 4-5 spectral bands	Band 6 and for Landsat MSS 1-3. Band 3 for Landsat MSS 4-5 spectral bands	18
Landsat 4–5	30–120	1991, 2001, and 2011	TM	7	Ended in 2013	Band 2	Band 4	16
Landsat 7	15–60	2001, 2011, and 2021	ETM +	7	Operational	Band 2	Band 4	16
Landsat 8-9	30–100	2021	OLI and TIRS	11	Operational	Band 3	Band 5	16
Sentinel-2	10–60	2021	MSI	13	Operational	Band 3	Band 8	10

Table 2 The coefficient of coastal armouring K computed for each segment for the 1972 and the 2021. The total length of the shoreline (L) and the armoured coast length (*l*) per year are shown. All measures are expressed in meters (m).

	Segment 1			**Segment 2**		
Year	**L**	***l***	**K**	**L**	***l***	**K**
1972	43761.9	23119.7	0.53	13175.5	1352.15	0.10
2021	58584.1	35232.8	0.60	17488.2	2058.04	0.12